

# A NUMERICAL METHOD FOR MODELLING THE MOTION OF A SPHERICAL BUBBLE

P. J. HARRIS

*Department of Mathematical Sciences, Watts Building, University of Brighton, Lewes Road, Brighton, U.K.*

## SUMMARY

This paper presents a numerical method for predicting the motion of a spherical bubble close to a rigid structure. The velocity potential in the fluid due to the motion of the bubble is represented by a source and a dipole located at the centroid of the bubble. This leads to a coupled system of differential equations for the bubble radius and the location of its centroid. This system of equations can be solved using an appropriate numerical scheme.

KEY WORDS: bubble dynamics; fluid–structure interaction; boundary integral method

## 1. INTRODUCTION

This paper is concerned with determining the motion of a bubble in a liquid close to a rigid structure through the use of an appropriate numerical model. Previous work on this problem has been concentrated on two main methods: the boundary integral (or element) method and the point source or spherical bubble method. Both these methods have their advantages and disadvantages.

The boundary integral method has been shown to be a powerful tool for solving exterior boundary value problems in unbounded domains (see e.g. References 1 and 2). The method has been successfully used to model the motion of axisymmetric bubbles close to horizontal rigid planes and free surfaces.<sup>3,4</sup> Using such axisymmetric models, it is possible to predict the motion of the bubble after the jet, which forms during the bubble collapse, has impacted on the opposite side of the bubble.<sup>5</sup> However, for a fully three-dimensional model it is not clear how to detect the point or time of the jet impact. In addition, the simple time-stepping schemes, such as the Euler method, used in order to reduce the computational cost appear to be unstable, leading to inaccurate results, although such methods have been used with some success in predicting the motion of the bubble during its growth phase and the early stages of its collapse.<sup>6–9</sup>

The alternative method of solution, the point source method, is not as detailed as the boundary integral method in that it does not provide any information about either the bubble shape or the bubble migration. However, it is possible to compute the Kelvin impulse of the bubble, which can be used as an indication of the direction of the bubble jet. This method has been used to predict the direction of the bubble jet in a number of situations, such as bubbles close to rigid planes, spheres, cylinders and slender bodies.<sup>5,10,11</sup> This method has the advantage that it is computationally cheap and the time stepping is stable.

This paper extends the point source method by using both a point source and a dipole at the bubble centroid to describe the fluid motion. By assuming that the bubble remains spherical, it is possible to model the motion of the bubble due to buoyancy and other forces which may be acting on the bubble.

Such models could be of use in situations where the shape of the bubble is not of primary interest but the effect of the bubble on a near-by structure is. As the bubble oscillates, it will cause high- and low-pressure points to occur on the surface of the structure and the location and magnitude of these may change as the location of the bubble centroid changes.

## 2. MATHEMATICAL MODEL

### 2.1. Bubble in an unbounded fluid

Assume that the fluid is inviscid, incompressible and irrotational. Then the fluid velocity is given by the gradient of a scalar potential which is the solution to Laplace's equation in the fluid domain. Following the analysis of Taylor,<sup>12</sup> assume that the bubble surface remains spherical and that the velocity potential due to the bubble can be modelled using a point source and a dipole at the bubble centroid  $\mathbf{p}_b$ . That is

$$\phi(\mathbf{p}) = \frac{m}{r} + \frac{\mathbf{G} \cdot \mathbf{r}}{r^3}, \quad (1)$$

where  $m$  and  $\mathbf{G}$  are the source and dipole strengths respectively and  $\mathbf{r} = \mathbf{p} - \mathbf{p}_b$ , with  $r = |\mathbf{r}|$ . The motion of the bubble can be described as spherically symmetric expansion and contraction added to the rigid body translation of a sphere. The radial motion of the bubble expansion and collapse leads to the source strength being given by<sup>13,14</sup>

$$m = -R^2 \dot{R}, \quad (2)$$

where  $R$  is the bubble radius and an overdot denotes differentiation with respect to time. The instantaneous rigid body translation of the sphere leads to the components of the dipole strength as<sup>13</sup>

$$G_x = -\frac{R^3 u_x}{2}, \quad G_y = -\frac{R^3 u_y}{2}, \quad G_z = -\frac{R^3 u_z}{2}, \quad (3)$$

where  $u_x$ ,  $u_y$  and  $u_z$  are the components of the velocity of the bubble centroid. Thus

$$\phi(\mathbf{p}) = -\frac{R^2 \dot{R}}{r} - \frac{R^3 \mathbf{u} \cdot \mathbf{r}}{2r^3}. \quad (4)$$

The kinetic energy of the bubble is given by<sup>13,14</sup>

$$K = \frac{\rho}{2} \int_S \phi \frac{\partial \phi}{\partial \mathbf{n}} dS, \quad (5)$$

where  $S$  is the surface of the bubble (with unit normal  $\mathbf{n}$ ) and  $\rho$  is the density of the fluid. The rate of change of the kinetic energy is equal to the rate of work being done on the fluid.<sup>13</sup> Thus

$$\frac{dK}{dt} = 4\pi(p_b - p_\infty + \rho g z_b) R^2 \dot{R} - \frac{4\pi}{3} u_z \rho g, \quad (6)$$

where  $p_b$  and  $p_\infty$  are the internal pressure of the bubble and the far-field pressure in the plane  $z = 0$  respectively. Here  $g$  is the acceleration due to gravity, which is assumed to be directed along the negative  $z$ -axis. Substituting in (4) yields

$$R\ddot{R} = \frac{p_b - p_\infty + \rho g z_b}{\rho} - \frac{R u_z g}{3\dot{R}} - \frac{3}{2} \dot{R}^2 + \frac{R \mathbf{u} \cdot \dot{\mathbf{u}}}{6\dot{R}} + \mathbf{u} \cdot \mathbf{u}. \quad (7)$$

If the bubble centroid is assumed to be stationary, then the components of the velocity  $\mathbf{u}$  are all equal to zero and (7) becomes the well-known Rayleigh–Plesset equation.

The Kelvin impulse of the bubble is given by<sup>14</sup>

$$\mathbf{I} = \rho \int_s \phi \mathbf{n} dS \quad (8)$$

and the rate of change of the Kelvin impulse is equal to the applied forces.<sup>13</sup> That is

$$\frac{d\mathbf{I}}{dt} = \mathbf{F}(t) \quad (9)$$

and differentiating (8) yields

$$\mathbf{F} = \frac{2\pi\rho}{3} (3R^2 \dot{R}\mathbf{u} + R^3 \ddot{\mathbf{u}}). \quad (10)$$

Since only buoyancy forces are acting on the bubble, it follows that the components of  $\mathbf{F}$  are  $F_x = F_y = 0$  and  $F_z = 4\pi\rho gR^3/3$ . Using (10) to eliminate  $\ddot{\mathbf{u}}$  from (7) yields

$$R\ddot{R} = \frac{P_b - P_\infty + \rho g z_b}{\rho} - \frac{3}{2}\dot{R}^2 - \frac{1}{2}|\mathbf{u}|^2. \quad (11)$$

## 2.2. Bubble in a fluid near a rigid structure

For a bubble in a fluid near to some form of rigid structure the velocity potential can be expressed as the sum of the potential due to the bubble,  $\phi_b$ , and the potential due to the structure,  $\phi_s$  (i.e.  $\phi = \phi_b + \phi_s$ ). In order to derive an equation for the bubble radius, it is assumed that  $\phi_s$  on the surface of the bubble can be approximated by the value of  $\phi_s$  at the bubble centroid. This approximation is valid provided that the bubble is not too close to the structure. At the bubble centroid the potential  $\phi_s$  and its space derivatives can be expressed in terms of the source and dipole strengths of the bubble potential in the form

$$\begin{aligned} \phi_s &= a_0 m + a_1 G_x + a_2 G_y + a_3 G_z, & \frac{\partial \phi_s}{\partial x} &= b_0 m + b_1 G_x + b_2 G_y + b_3 G_z, \\ \frac{\partial \phi_s}{\partial y} &= c_0 m + c_1 G_x + c_2 G_y + c_3 G_z, & \frac{\partial \phi_s}{\partial z} &= d_0 m + d_1 G_x + d_2 G_y + d_3 G_z, \end{aligned} \quad (12)$$

where the time-dependent parameters  $a_0$  to  $d_3$  are determined from the geometry of the problem under consideration.

For simple geometries it is possible to determine these constants analytically using the method of images. For example, when considering a bubble close to a vertical rigid plane, all the parameters are zero except for

$$\begin{aligned} a_0 &= \frac{1}{2y_b}, & a_2 &= -\frac{1}{4y_b^2}, & b_1 &= \frac{1}{8y_b^3}, \\ c_0 &= -\frac{1}{4y_b^2}, & c_2 &= \frac{1}{4y_b^3}, & d_3 &= \frac{1}{8y_b^3}, \end{aligned} \quad (13)$$

where  $y = 0$  is the equation of the rigid plane and  $y_b$  is the  $y$ -co-ordinate of the bubble centroid. In this case the required time derivatives of these parameters can be obtained either analytically or by using a finite difference scheme.

For a bubble near a finite rigid structure, such as a sphere or a cylinder, the constants can be determined using the boundary integral method. Assume that the velocity potential due to the structure can be represented as a layer density over the structure surface.<sup>15</sup> That is

$$\phi_s(\mathbf{p}) = \int_{\Sigma} G(\mathbf{p}, \mathbf{q})\sigma(\mathbf{q}) dS_{\mathbf{q}} = A(\mathbf{p})\sigma, \quad (14)$$

where  $\sigma$  is the source density function. If  $\mathbf{p} \in \Sigma$ , then

$$\frac{\partial\phi_s}{\partial\mathbf{n}}(\mathbf{p}) = -\frac{\sigma(\mathbf{p})}{2} + \int_{\Sigma} \frac{\partial G}{\partial\mathbf{n}}(\mathbf{p}, \mathbf{q})\sigma(\mathbf{q}) dS_{\mathbf{q}} = (-\frac{1}{2}I + B)\sigma. \quad (15)$$

On the surface of the structure there is the boundary condition

$$\frac{\partial\phi}{\partial\mathbf{n}} = \frac{\partial\phi_s}{\partial\mathbf{n}} + \frac{\partial\phi_b}{\partial\mathbf{n}} = 0. \quad (16)$$

Thus

$$\phi_s = -A(-\frac{1}{2}I + B)^{-1} \frac{\partial\phi_b}{\partial\mathbf{n}}. \quad (17)$$

Since  $\phi_b$  (and hence  $\partial\phi_b/\partial\mathbf{n}$ ) is given by (1), then

$$\frac{\partial\phi_b}{\partial\mathbf{n}} = m \frac{\partial}{\partial\mathbf{n}} \left( \frac{1}{r} \right) + G_x \frac{\partial}{\partial\mathbf{n}} \left( \frac{x-x_b}{r^3} \right) + G_y \frac{\partial}{\partial\mathbf{n}} \left( \frac{y-y_b}{r^3} \right) + G_z \frac{\partial}{\partial\mathbf{n}} \left( \frac{z-z_b}{r^3} \right), \quad (18)$$

which leads to  $\phi_s$  in the form (12) with

$$\begin{aligned} a_0 &= -A(-\frac{1}{2}I + B)^{-1} \frac{\partial}{\partial\mathbf{n}} \left( \frac{1}{r} \right), & a_1 &= -A(-\frac{1}{2}I + B)^{-1} \frac{\partial}{\partial\mathbf{n}} \left( \frac{x-x_b}{r^3} \right), \\ a_2 &= -A(-\frac{1}{2}I + B)^{-1} \frac{\partial}{\partial\mathbf{n}} \left( \frac{y-y_b}{r^3} \right), & a_3 &= -A(-\frac{1}{2}I + B)^{-1} \frac{\partial}{\partial\mathbf{n}} \left( \frac{z-z_b}{r^3} \right). \end{aligned} \quad (19)$$

The space derivatives of  $\phi_s$ , which are needed at the bubble centroid, can be expressed as

$$\frac{\partial\phi_s}{\partial x} = -A_x(-\frac{1}{2}I + B)^{-1} \frac{\partial\phi_b}{\partial\mathbf{n}}, \quad (20)$$

where

$$A_x\sigma = \int_{\Sigma} \frac{\partial G}{\partial x} \sigma dS_{\mathbf{q}}, \quad (21)$$

which in turn yields

$$\begin{aligned} b_0 &= -A_x(-\frac{1}{2}I + B)^{-1} \frac{\partial}{\partial\mathbf{n}} \left( \frac{1}{r} \right), & b_1 &= -A_x(-\frac{1}{2}I + B)^{-1} \frac{\partial}{\partial\mathbf{n}} \left( \frac{x-x_b}{r} \right), \\ b_2 &= -A_x(-\frac{1}{2}I + B)^{-1} \frac{\partial}{\partial\mathbf{n}} \left( \frac{y-y_b}{r} \right), & b_3 &= -A_x(-\frac{1}{2}I + B)^{-1} \frac{\partial}{\partial\mathbf{n}} \left( \frac{z-z_b}{r} \right). \end{aligned} \quad (22)$$

It is possible to obtain similar expressions for the other constants  $c_0$  to  $d_3$  by introducing the integral operators  $A_y$  and  $A_z$  which are defined by replacing the  $x$ -derivative in (21) by a  $y$ - and a  $z$ -derivative respectively.

For problems involving a bubble near a finite rigid structure, it is not possible in general to find the derivative of the constants  $a_0$  and  $d_3$  analytically and so it is necessary to employ a finite difference scheme.

Once the parameters dependent on the geometry have been found, the kinetic energy can be determined using<sup>13</sup>

$$K = \int_S (\phi_b + \phi_s)(\nabla\phi_b + \nabla\phi_s)\mathbf{n} dS. \quad (23)$$

By using an approximation of the form (12) for  $\phi_s$  and its space derivatives and assuming that the bubble is spherical, (23) yields

$$\begin{aligned} K = & \rho\pi(2R^3\dot{R} + \frac{1}{3}R^3\mathbf{u}\cdot\mathbf{u} - \frac{1}{3}R^5\dot{R}(b_0u_x + c_0u_y + d_0u_z) \\ & - \frac{R^5\dot{R}}{2}[u_x(b_1u_x + c_1u_y + d_1u_z) + u_y(b_2u_x + c_2u_y + d_2u_z) + u_z(b_3u_x + c_3u_y + d_3u_z)] \\ & \times R^4\dot{R}(a_0\dot{R} + a_1Ru_x + a_2Ru_y + a_3Ru_z)). \end{aligned} \quad (24)$$

Since  $dK/dt$  equals the rate of work being done, the equation above can be differentiated to give a second-order ordinary differential equation for the bubble radius (see Appendix).

The acceleration of the bubble centroid can be calculated from (10) as

$$\dot{\mathbf{u}} = \frac{3}{2\pi\rho R^3}\mathbf{F} - \frac{3\dot{R}}{R}\mathbf{u}. \quad (25)$$

The forces  $\mathbf{F}$  acting on the bubble are given by<sup>16</sup>

$$\mathbf{F} = \rho \int_{\Sigma} \left( \frac{1}{2}|\nabla\phi|^2\mathbf{n} - \frac{\partial\phi}{\partial\mathbf{n}}\nabla\phi \right) dS, \quad (26)$$

where  $\Sigma$  denotes all surfaces bounding the fluid except the surface of the bubble.

The system of ordinary differential equations formed by considering the equation for the bubble radius (see Appendix), the equation for the velocity of the bubble centroid (25) and

$$\dot{\mathbf{p}}_b = \mathbf{u} \quad (27)$$

for the location of the bubble centroid  $\mathbf{p}_b$  can be integrated using an appropriate numerical scheme subject to suitable initial conditions.

Once the potential has been determined, it is possible to calculate the pressure distribution on the surface of the structure using Bernoulli's equation:<sup>14</sup>

$$p = p_{\infty} - \rho \frac{\partial\phi}{\partial t} - \rho \frac{1}{2}|\nabla\phi|^2 - \rho gz. \quad (28)$$

The initial conditions for the system are that the bubble radius, radial velocity and location are specified. The initial velocity of the bubble centroid is assumed to be zero. Therefore, since the structure is assumed to be stationary, it follows that the time derivatives of the constants  $a_0$  to  $d_3$  are all initially zero.

### 2.3. Numerical methods

For a bubble close to an infinite rigid plane the constants  $a_0$  to  $d_3$  can be computed analytically and the resulting system of coupled ordinary differential equations can be solved using a fourth-order Runge-Kutta scheme.<sup>17</sup> However, for a bubble near a finite rigid structure the constants  $a_0$  to  $d_3$  need to be determined numerically by solving the integral equations appearing in (24) (and the similar integral equations which appear in the expressions for the constants  $b_0$  to  $d_3$ ). In this work all these integral equations are solved via the boundary element method using a piecewise constant approximation to the source density. Full details of such boundary element methods for Laplace's (or related) equations can

be found in References 1, 18 and 19 for example. The use of the piecewise constant approximation avoids the problem of the surface not having well-defined normals at the nodal points, since element centroids are taken as the collocation points.

It is noted that the approximation to  $(-\frac{1}{2}I + B)^{-1}$  only needs to be computed once, since the structure is rigid and fixed. However, the approximations to the integral operators  $A$ ,  $A_x$ ,  $A_y$  and  $A_z$  need to be computed at each step as they depend on the relative locations of the bubble and the structure.

The potential at the nodal points of the surface of the structure, needed for pressure calculation, can be computed from (1) and (17) with  $\mathbf{p} \in \Sigma$ . The gradient of the potential on the surface of the structure could be computed using (20), but there are numerical problems with doing this due to the singularities in the kernel functions of the integral operators  $A_x$ ,  $A_y$  and  $A_z$ . Alternatively, the gradient of the potential can then be computed using the combined finite difference and least squares scheme introduced by Harris.<sup>9</sup> The time derivative of the potential can be found by differentiating (1) and (17) and using finite differences where appropriate.

The timestep can be allowed to vary in length. When the bubble is close to its maximum radius, the physical quantities are changing slowly with time so it is possible to take larger time steps, but when the bubble is close to its minimum radius, the physical quantities are changing more rapidly with time and it is necessary to take smaller time steps. Here the time steps are calculated using

$$\delta t = \delta t_0 R(t), \quad (29)$$

where  $\delta t_0$  is a specified parameter. This scheme gives larger time steps when the bubble has a larger radius and appears to give a stable time-stepping method.

### 3. NUMERICAL RESULTS

The results discussed in this section are for bubbles in a number of typical situations. It should be noted that these results were obtained using the non-dimensional form of the governing equations. Here the length scale is  $R_{\max}$ , the maximum radius of the bubble, the time scale is  $R_{\max} \sqrt{(\Delta p / \rho)}$  and the pressure scale  $\Delta p$  is chosen such that  $p_\infty = 1$ . Full details of the non-dimensional variables can be found in Reference 3.

Figure 1 shows the bubble radius and horizontal and vertical displacements for a bubble 5 units from a vertical rigid wall. The horizontal displacement is towards the rigid wall and the vertical motion is upwards owing to the buoyancy of the bubble. Figure 2 shows the corresponding results for a bubble 10 units from the boundary. These results illustrate that the bubble is attracted towards the rigid boundary and that the force of attraction is greater for bubbles which are closer to the vertical wall. However, the vertical motion due to buoyancy is almost unaffected by the distance of the bubble from the rigid wall. These results also show that the distance from the wall has a small effect on the radius of the bubble. The bubble furthest from the wall has a slightly shorter period of oscillation.

Figures 3 and 4 show the pressure on the surface of a rigid cylinder for the same bubble at different times. These results show that there is a high-pressure region on the surface of the cylinder whenever the bubble is close to its minimum radius. Further, as the bubble rises owing to buoyancy, the location of the high-pressure region moves up the side of the cylinder. These repeated high-pressure pulses generated by the oscillating bubble could be a mechanism for damage to an elastic structure. Figure 5 shows the location of the bubble centroid to the location of the cylinder. This shows how the bubble migrates towards the structure.

Figure 6 shows that variation in the pressure at a point on a rigid sphere with a bubble immediately above and Figure 7 shows the bubble radius. Clearly there are sharp peaks in the pressure whenever the bubble reaches its minimum volume, but as the bubble rises away from the sphere, the level of the peaks is decreasing.

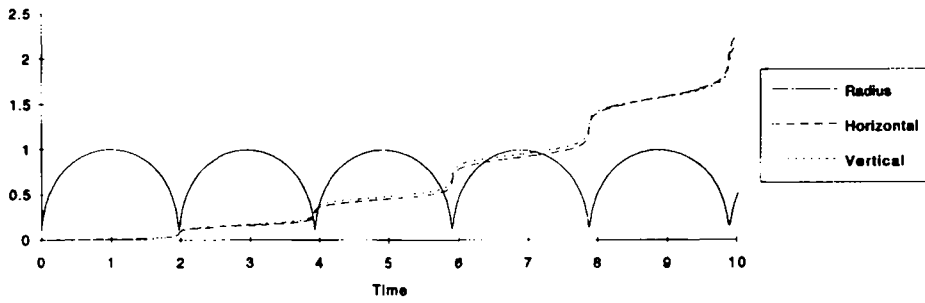


Figure 1. Bubble radius and horizontal and vertical displacements for a bubble 5 units from a vertical rigid wall

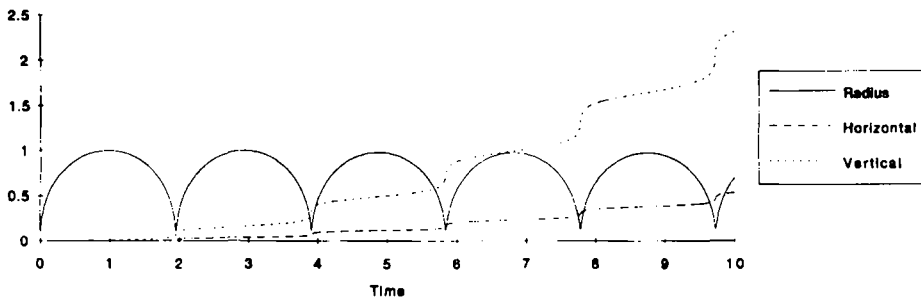
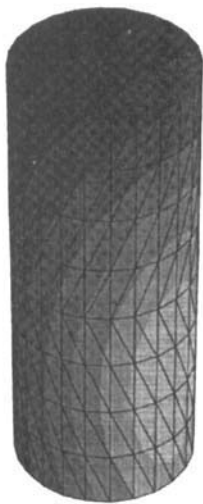


Figure 2. Bubble radius and horizontal and vertical displacements for a bubble 10 units from a vertical rigid wall



■	9.06287 to	9.56907
■	8.55667 to	9.06287
■	8.05046 to	8.55667
■	7.54426 to	8.05046
■	7.03806 to	7.54426
■	6.53185 to	7.03806
■	6.02565 to	6.53185
■	5.51945 to	6.02565

Figure 3. Pressure distribution on the surface of a cylinder early in the bubble's lifetime

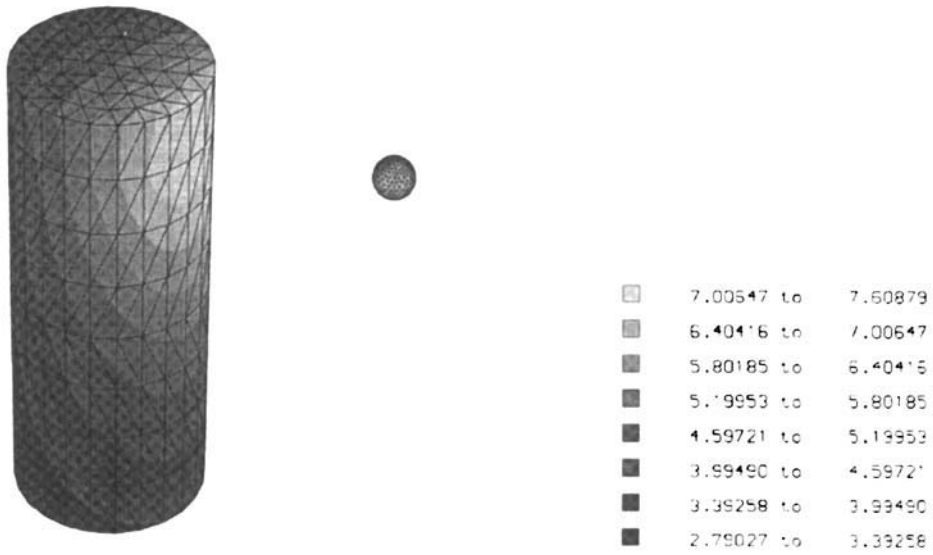


Figure 4. Pressure distribution on the surface of a cylinder later in the bubble's lifetime

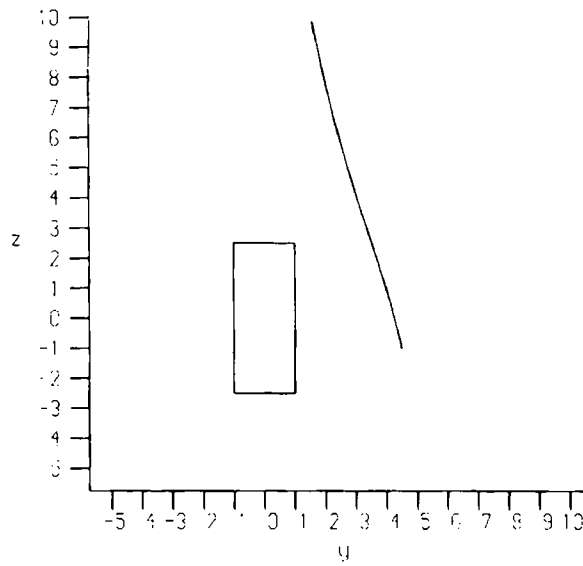


Figure 5. Change in location of bubble centroid

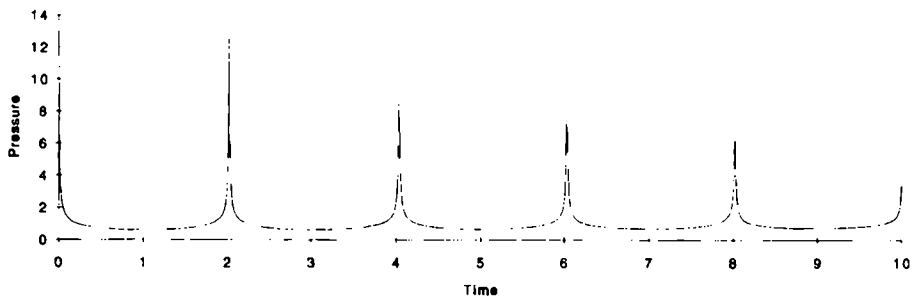


Figure 6. Pressure on the surface of a sphere at the point closest to the initial bubble

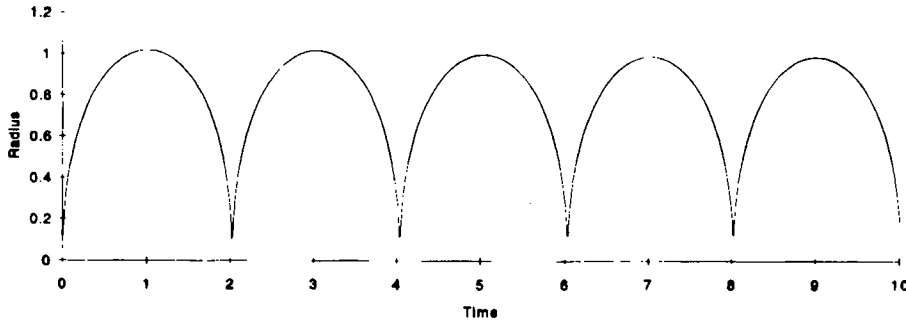


Figure 7. Radius of a bubble above a rigid sphere

4. CONCLUSIONS

The present model is an effective numerical method for studying the effect of a bubble on a near-by structure. The full boundary integral method considered in References 8 and 9 can only effectively consider the motion over the first bubble growth and the early stages of the subsequent collapse before the time stepping becomes unstable. The point source method can model a number of bubble oscillations, but is limited because the location of the bubble centroid does not change. The model proposed here can be used to study the effects of the bubble on the structure over a number of bubble oscillations. This model has the additional advantage over the full boundary integral method that it is relatively cheap in terms of computer CPU time.

ACKNOWLEDGEMENTS

This work was funded in part by the Defence Research Agency, Fort Halstead, Sevenoaks, Kent, U.K. The author would also like to acknowledge the help and advice of Professor John Blake, University of Birmingham.

APPENDIX

The ordinary differential equation for the bubble radius is

$$\begin{aligned} & \ddot{R} [4R^3 - \frac{1}{3}R^5(b_0u_x + c_0u_y + d_0u_z)] / \dot{R} + R^4(a_0\dot{R} + a_1Ru_x + a_2Ru_y + a_3Ru_z) / \dot{R} + R^4a_0] \\ & = 4R^2(p_b - p_\infty + \rho gz_b) / \rho - 4u_zg / 3\dot{R} - 6R^2\ddot{R} - 2R^3(u_x\dot{u}_x + u_y\dot{u}_y + u_z\dot{u}_z) / 3\dot{R} \\ & + 5R^4\dot{R}(b_0u_x + c_0u_y + d_0u_z) / 3 + R^5(b_0\dot{u}_x + c_0\dot{u}_y + d_0\dot{u}_z + \dot{b}_0u_x + \dot{c}_0u_y + \dot{d}_0u_z) / 3 \\ & + (R^6\dot{u}_x / \dot{R} + 6R^5u_x)(b_1u_x + c_1u_y + d_1u_z) / 2 + R^6u_x(b_1\dot{u}_x + c_1\dot{u}_y + d_1\dot{u}_z + \dot{b}_1u_x + \dot{c}_1u_y + \dot{d}_1u_z) / 2\dot{R} \\ & + (R^6\dot{u}_y / \dot{R} + 6R^5u_y)(b_2u_x + c_2u_y + d_2u_z) / 2 + R^6u_y(b_2\dot{u}_x + c_2\dot{u}_y + d_2\dot{u}_z + \dot{b}_2u_x + \dot{c}_2u_y + \dot{d}_2u_z) / 2\dot{R} \\ & + (R^6\dot{u}_z / \dot{R} + 6R^5u_z)(b_3u_x + c_3u_y + d_3u_z) / 2 + R^6u_z(b_3\dot{u}_x + c_3\dot{u}_y + d_3\dot{u}_z + \dot{b}_3u_x + \dot{c}_3u_y + \dot{d}_3u_z) / 2\dot{R} \\ & - 4R^3\dot{R}(a_0\dot{R} + a_1Ru_x + a_2Ru_y + a_3Ru_z) - R^4(\dot{a}_0\dot{R} + a_1\dot{R}u_x + a_1Ru_x + \dot{a}_1Ru_x \\ & + a_2\dot{R}u_y + a_2Ru_y + \dot{a}_2Ru_y + a_1\dot{R}u_z + a_3Ru_z + \dot{a}_3Ru_z). \end{aligned}$$

It is noted that if the bubble's initial radial velocity is zero, then there appears to be a problem with dividing by  $\dot{R}$ . However, the initial conditions require that all the terms divided by  $\dot{R}$  are initially zero. Although it is possible to get  $\dot{R} = 0$  at some subsequent point in the calculation, there is very unlikely and can overcome by setting  $\dot{R}$  to be some small but non-zero value.

## REFERENCES

1. S. Amini, P. J. Harris and D. T. Wilton, *Lecture Notes in Engineering*, Vol. 77, *The Coupled Boundary and Finite Element Methods for the Solution of the Dynamic Fluid-Structure Interaction Problem*, Springer, Berlin, 1992.
2. K. E. Atkinson, 'The numerical solution of Laplace's equation in three dimensions', *SIAM J. Numer. Anal.*, **19**, 263-274 (1982).
3. J. R. Blake, B. B. Taib and G. Doherty, 'Transient cavities near boundaries. Part 1, Rigid boundaries', *J. Fluid Mech.*, **170**, 479-497 (1986).
4. J. R. Blake, B. B. Taib and G. Doherty, 'Transient cavities near boundaries. Part 2. Free surface', *J. Fluid Mech.*, **181**, 197-212 (1987).
5. J. P. Best, 'The dynamics of underwater explosions', *Ph.D. Thesis*, University of Wollongong, 1991.
6. G. L. Chahine and T. O. Perdue, 'Simulation of the three-dimensional behaviour of an unsteady large bubble near a structure', *Proc. 3rd Int. Colloq. on Bubbles and Drops*, AIP conference proceedings **197**, pp 188-199, Monterey, CA, 1988.
7. G. L. Chahine, 'A numerical model for three-dimensional bubble dynamics in complex flow configurations', *Rep. 6.002-2*, Dynaflo Inc., Laurel, MD, 1989.
8. P. J. Harris, 'A numerical model for determining the motion of a bubble close to a fixed rigid structure in a fluid', *Int. j. numer. methods eng.*, **33**, 1813-1822 (1992).
9. P. J. Harris, 'A numerical method for predicting the motion of a bubble close to a moving rigid structure', *Commun. Appl. Numer. Methods*, **9**, 81-86 (1993).
10. J. P. Best and J. R. Blake, 'An estimate of the Kelvin impulse of a transient cavity', *J. Fluid Mech.*, **261**, 75-93 (1992).
11. P. J. Harris, 'The numerical determination of the Kelvin impulse of a bubble close to a submerged rigid structure', *Comp. Meth. Appl. Mech. Eng.* in press (1996).
12. G. I. Taylor, *Scientific Papers*, Vol. 3, 1963, p. 320.
13. G. K. Batchelor, *An Introduction to Fluid Dynamics*, Cambridge University Press, Cambridge, 1967.
14. J. Lighthill, *An Informal Introduction to Theoretical Fluid Mechanics*, Oxford University Press, Oxford, 1986.
15. M. A. Jaswon and G. T. Symm, *Integral Equation Methods in Potential Theory and Elastostatics*, Academic, London, 1977.
16. J. R. Blake, 'The Kelvin impulse: applications to cavitation bubble dynamics', *J. Aust. Math. Soc. B*, **30**, 127-146 (1988).
17. K. E. Atkinson, *An Introduction to Numerical Analysis*, Wiley, New York, 1988.
18. K. E. Atkinson, *A Survey of Numerical Methods for the Solution of Fredholm Integral Equations of the Second Kind*, SIAM, Philadelphia, PA, 1976.
19. L. M. Delves and J. L. Mohamed, *Computational Method for Integral Equations*, Cambridge University Press, Cambridge, 1985.